ORIGINAL ARTICLE

JBMR®

Association of QCT Bone Mineral Density and Bone Structure With Vertebral Fractures in Patients With Multiple Myeloma

Jan Borggrefe,[1,2] Sarah Giravent,[1] Felix Thomsen,[1,3] Jaime Peña,[1] Graeme Campbell,[1] Asmus Wulff,[1] Andreas Günther,[4] Martin Heller,[1] and Claus C Glüer[1]

[1]Section for Biomedical Imaging, Department of Radiology and Neuroradiology, University-Clinics Schleswig Holstein, Campus Kiel, Kiel, Germany

[2]Institute for Diagnostic and Interventional Radiology, University-Clinics Cologne, Cologne, Germany

[3]Department of Engineering, National University of the South, Bahia Blanca, Argentina

[4]Section for Immun- and Stemcell- Therapy, Department of Inner Medicine, University-Clinics Schleswig Holstein, Campus Kiel, Kiel, Germany

ABSTRACT

Computed tomography (CT) is used for staging osteolytic lesions and detecting fractures in patients with multiple myeloma (MM). In the OsteoLysis of Metastases and Plasmacell-infiltration Computed Tomography 2 study (OLyMP-CT) study we investigated whether patients with and without vertebral fractures show differences in bone mineral density (BMD) or microstructure that could be used to identify patients at risk for fracture. We evaluated whole-body CT scans in a group of 104 MM patients without visible osteolytic lesions using an underlying lightweight calibration phantom (Image Analysis Inc., Columbia, KY, USA). QCT software (Structural*Insight*) was used for the assessment of BMD and bone structure of the T_{11} or T_{12} vertebral body. Age-adjusted standardized odds ratios (sORs) per SD change were derived from logistic regression analyses, and areas under the receiver operating characteristics (ROC) curve (AUCs) analyses were calculated. Forty-six of the 104 patients had prevalent vertebral fractures (24/60 men, 22/44 women). Patients with fractures were not significantly older than patients without fractures (mean $\pm$ SD, 64 ± 9.2 versus 62 ± 12.3 years; $p = 0.4$). Trabecular BMD in patients with fractures versus without fractures was 169 ± 41 versus 192 ± 51 mg/cc (AUC $= 0.62 \pm 0.06$, sOR $= 1.6$ [1.1 to 2.5], $p = 0.02$). Microstructural variables achieved optimal discriminatory power at bone thresholds of 150 mg/cc. Best fracture discrimination for single microstructural variables was observed for trabecular separation (Tb.Sp) (AUC $= 0.72 \pm 0.05$, sOR $= 2.4$ (1.5 to 3.9), $p < 0.0001$). In multivariate models AUCs improved to 0.77 ± 0.05 for BMD and Tb.Sp, and 0.79 ± 0.05 for Tb.Sp and trabecular thickness (Tb.Th). Compared to BMD values, these improvements of AUC values were statistically significant ($p < 0.0001$). In MM patients, QCT-based analyses of bone structure derived from routine CT scans permit discrimination of patients with and without vertebral fractures. Rarefaction of the trabecular network due to plasma cell infiltration and osteoporosis can be measured. Deterioration of microstructural measures appear to be of value for vertebral fracture risk assessment and may indicate early stages of osteolytic processes not yet visible. © 2014 American Society for Bone and Mineral Research.

KEY WORDS: MULTIPLE MYELOMA; OSTEOPOROSIS; VERTEBRAL FRACTURE; QCT; FRACTURE RISK; TRABECULAR SEPARATION; BMD

Introduction

Multiple myeloma (MM) is a low-grade B-cell non-Hodgkin lymphoma, which is characterized by a proliferation of monoclonal malignant plasma cells. The incidence of the disease amounts to approximately 1% of all malignant neoplasms.[1] MM is associated with diffuse and focal lytic bone destruction and osteoporosis in 80% of patients.[2] These changes lead to a high incidence of fracture, of which vertebral compression fractures are the most common, occurring in 20% to 70% of patients.[3–7] Vertebral fractures in MM patients are associated with a high impairment of quality of life, morbidity, and mortality.[5,8] Multiple treatment regimens targeted at reducing fracture incidence have been introduced in the last decade or are currently under development.[9–15] To facilitate drug development, radiologists are asked to provide detailed reports regarding changes induced by treatment effects or progression of MM disease. Specifically, the risk of imminent fracture is of particular interest, in order to make a decision whether to refer to surgical treatment, vertebroplasty, or radiotherapy.[15,16] However, the criteria used to define impaired stability of vertebral bodies are not clearly defined. Some authors suggest the number of focal lesions as indicator for diffuse bone infiltration[17] or cortical erosion as a major threat for vertebral

Received in original form July 24, 2014; revised form September 8, 2014; accepted September 16, 2014. Accepted manuscript online December 26, 2014.
Address correspondence to: Jan Borggrefe, Kerpenerstr.62, 50935 Köln, Germany. E-mail: jan.borggrefe@uk-koeln.de

Journal of Bone and Mineral Research, Vol. 30, No. 7, July 2015, pp 1329–1337
DOI: 10.1002/jbmr.2443
© 2014 American Society for Bone and Mineral Research

fractures.[15] Other recommendations are based on the clinical experience of orthopedic surgeons, that an osteolytic lesion larger than 50% of the vertebral body is associated with severe fracture risk.[18,19] However, these crude criteria for focal osteolytic events lack the backup of longitudinal individualized biomechanical investigations, eg, based on finite element modeling, which have become technically feasible with recent developments of CT technology.[20–23] Focal large osteolytic lesions detectable by the clinician may not be sensitive enough to reflect the most common cause of vertebral fractures in MM patients; ie, diffuse osteopenia caused by the disease and other factors.

To address these issues, high-resolution QCT (HR-QCT) of the vertebrae, as suggested by several authors[20–22] including Takasu and colleagues,[23] may provide valuable insight into the microstructural changes in the lumbar spine of myeloma patients. Common low-dose spiral CT appears to be a promising approach for a comprehensive assessment of the entire spine. In this cross-sectional study, we tested the performance of a low-dose structural analysis (LDSA) protocol to investigate the vertebral body T_{11} or T_{12} as part of a routine low-dose whole-body scan for discriminating patients with and without prevalent vertebral fractures. LDSA might offer a sensitive new method to assess early microstructural changes in trabecular bone caused by MM, and the effect of those changes on bone fragility. This in turn may have clinical benefit by permitting a more sensitive and objective way of assessing indications for preventive measures in patients at risk for fracture and neural complications.

Patients and Methods

Study design and participants

In this OsteoLysis of Metastases and Plasmacell-infiltration Computed Tomography 2 (OLyMP CT) study population, we recruited 178 patients referred to the Department of Diagnostic Radiology, UKSH Campus Kiel, for non–contrast-enhanced CT scans with the indication of staging for myeloma. In a cross-sectional analysis, the first CT scan for each patient between January 2010 and January 2012 was examined. All patients with myeloma had received thalidomide treatment preceding the study. The study was approved by the local ethics commission (registration ID: D 430/12) and was designed to meet good clinical practice (GCP) criteria. Patients were excluded from the investigation if they had not permitted data use for study purpose at admission or if they met the following exclusion criteria: previous malignant neoplasm, known metabolic bone disorders, history of sprue, abnormal thyroid or other clinical studies. All patients with a fracture of both T_{11} and T_{12} were excluded from the investigation. Fifty of 178 patients were excluded according to these criteria. Vertebral compression fractures were diagnosed according to the Genant criteria,[24] and were evaluated separately by two radiologists for this study (JB and AW), followed by a consensus check of all CT data including the initial clinical patient reports.

Scan protocol and bone densitometry

All patients were scanned on the same Siemens Somatom Sensation 64 row CT Scanner (Siemens, Forchheim, Germany). Scans of T_{12} (or of T_{11} in the case that the T_{12} was fractured or showed macroscopic evidence of osteolytic lesions) were conducted with the preexisting CT protocol of 120 kVp, 100 mA, and a 1.5-mm slice thickness, resulting in a dose of approximately 4.0 to 6.5 mSv (International Commission on Radiological Protection [IRCP] publication 103; http://www.icrp.org) (see Fig. 1). The InTable calibration phantom (Image Analysis Inc., Columbia, KY, USA) embedded in the CT mat underneath the patient (Fig. 2*A*, *B*) was included in all CT scans, thus permitting quantitative CT analyses. The CT data were

Fig. 1. (*A*) Example sagittal reformation from an LDSA scan of a patient with large osteolytic lesions as seen in T_{12}, but no vertebral fractures. (*B*) Example sagittal reformation from an LDSA scan of a patient with multiple fractures and diffuse osteolytic changes of the spine. Unfractured T_{11} was used for data analysis. Kyphoplasty of L_1 and L_3 was performed to stabilize fractures of these vertebrae. LDSA = low-dose structural analysis.

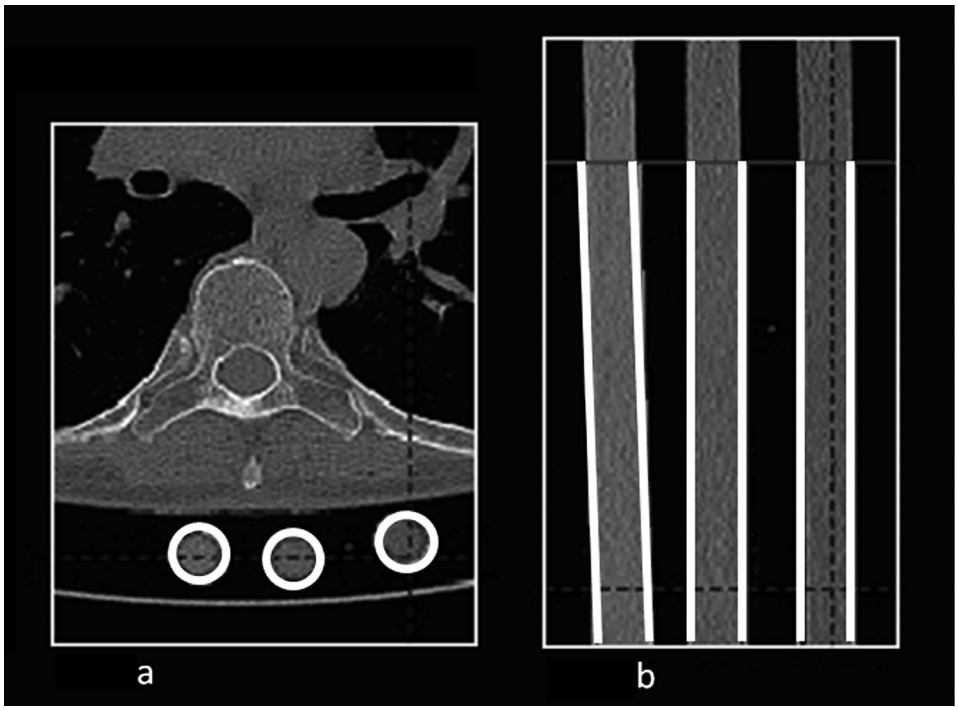

Fig. 2. LDSA of a vertebral body T_{11}. (*A*) Scan calibration with the in-house–developed QCT software Structural*Insight* (v.3.0) using the InTable calibration phantom (Image Analysis Inc., Columbia, KY, USA). (*B*) Adjustment for the discrete phantom tilt of the lightweight phantom of the left calibration pole. LDSA = low-dose structural analysis.

reconstructed with the B70s reconstruction kernel in two different formats: [1] a regular resolution reconstruction used for BMD calibration encompassing the entire cross-section of the patient and the calibration phantom underneath the patient (Fig. 2*A*) and [2] a higher resolution reconstruction (120 mm field of view [FOV], matrix size = 512 × 512 pixels) limited to the vertebral body for BMD and microstructural analyses (Fig. 3). Longitudinal quality assurance to ensure stability of the scanner throughout the study was performed using a Mindways Type 3 QA phantom and calibration phantom (Mindways, Austin, TX, USA). The in-house–developed QCT software Structural*Insight* (v.3.0), [25–28] was adapted to perform bone mineral calibration using the InTable phantom.

Cortical and trabecular bone were defined with semiautomatic bone segmentation. Bone was separated from marrow using a uniform threshold for all patients. To define the optimum protocol for the microstructural analysis and to test its robustness, the performance of all variables was evaluated for a range of thresholds between 80 and 500 mg/cc, centered at the established threshold for HR-QCT assessments[28] (Supporting Information). The vertically oriented cortex excluding the cortical endplates was segmented for a separate cortical analysis.

Bone microstructure was assessed by Structural*Insight*. Voxel-based bone volume fraction (BV/TV) and trabecular number (Tb.N), based on the direct secant method and using a parallel plate model, defined the trabecular thickness (Tb.Th), [29] while trabecular separation (Tb.Sp) using the run-length method[30] and vertical cortical thickness (Ct.Th) using the maximum-sphere method[31] were model-independent measures. A priori–defined primary outcome variables for this study were trabecular BMD, Tb.Sp, and Ct.Th, because these variables had proved to be useful in HR-QCT. In our HR-QCT experience T_{12} permits good quality imaging and yields valuable results, thus the lower thoracic level was chosen for this study as well. Secondary outcome variables included BV/TV, Tb.N, and Tb.Th. The data evaluation had been validated using a virtual phantom and by testing the method ex vivo.[32]

Statistical analysis

The statistical analysis was performed using JMP 9.0 software (SAS Institute, Cary, NC, USA). Descriptive statistics for normally distributed variables are presented as mean ± SD unless noted otherwise. Student's *t* tests were performed for assessing differences between groups. Standardized odds ratios (sORs) per standard deviation of the distribution of the patients without fractures and their 95% CIs were calculated from logistic regression analysis. Areas under the receiver operating characteristic (ROC) curve (AUCs) as well as significance of difference between ROC curves with the de Long method[33] were calculated using the software Medcalc 13.0.2 (MedCalc Software, Ostend, Belgium).

Results

Of the 128 patients included in the LDSA analysis, 13 patients were excluded in the outlier analysis due to beam hardening artifacts and protocol errors. Eleven patients were excluded due to diffuse osteolytic lesions of the entire spine that included T_{11} and T_{12}. The remaining patient group that met all study criteria consisted of 104 patients, 60 men and 44 women, aged 31 to 89 years (mean ± SD, 63 ± 11 years). The patient group included patients without osteolytic lesions that had been diagnosed to have monoclonal gammopathy of unknown significance

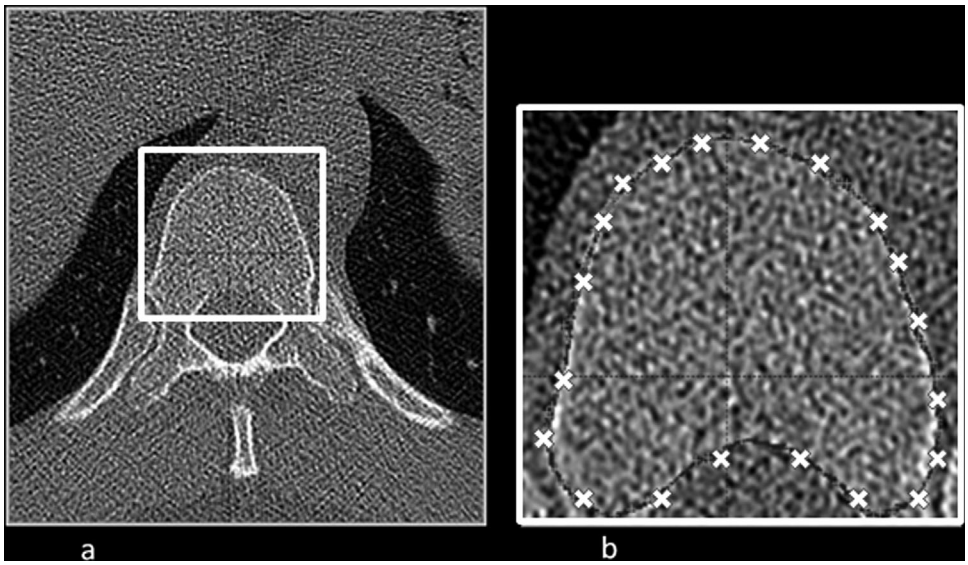

Fig. 3. LDSA of a vertebral body T_{11}. (*A*) A second higher resolution reconstruction of the vertebra with 512-pixel matrix of the spine was provided that was calibrated based on the scan data with phantom. (*B*) The vertebral body was segmented manually allowing separation of trabecular and cortical bone. LDSA = low-dose structural analysis.

(MGUS) ($n = 15$) or low-grade myeloma Salmon and Durie (S&D) grade 1 ($n = 12$). The majority of patients showed manifest and severe myeloma according to staging by S&D criteria (S&D grade 2: $n = 9$; S&D grade 3: $n = 68$).

The QCT measurements showed significant gender differences for cortical BMD (387 ± 6 mg/cc for men versus 365 ± 7 mg/cc for women, $p = 0.03$), for Tb.N (0.82 ± 0.006 vs 0.79 ± 0.007, $p = 0.005$) as well as a trend for Tb.Th (0.69 ± 0.016 versus 0.65 ± 0.014, $p = 0.06$).

BMD was significantly lower in fracture cases compared to controls (169.8 ± 40.5 versus 191.7 ± 50.6 mg/cc, $p = 0.003$). ROC and logistic regression confirmed these results (AUC = 0.66, sOR = 1.6 [1.1 to 2.5], $p < 0.01$). There was no significant impact or interaction effect of age or gender on fracture discrimination. The analysis was nevertheless conducted separately for men and women. We observed a trend to lower BMD in male versus female fracture patients (178 ± 34.6 versus 162 ± 44.5 mg/cc, $p = 0.17$). BMD results of fracture cases were significantly reduced compared to controls in men ($p = 0.02$), but not in women ($p = 0.3$). Similarly, ROC and logistic regression analysis of the association of BMD with fractures showed significant differences in men (AUC = 0.70 ± 0.07, sOR = 1.6 [1.1 to 2.5], $p < 0.02$) but not in women (AUC = 0.57 ± 0.09, sOR = 1.3 [0.7 to 2.5], $p = 0.3$).

Microstructural results strongly depended on the threshold for binarization of bone versus bone marrow. Therefore, we first had to determine the optimum threshold. Figure 4 shows the AUCs for the discriminatory power derived from logistic regression analysis for the main microstructural variables, depicted for bone thresholds in the range of 80mg/cc to 500mg/cc. In men, Tb.Sp showed optimal performance to distinguish patients with and without fractures with the use of thresholds between 80 – 200 mg/cc (AUC 0.75 - 0.80). In women, Tb.Sp performed best with the use of thresholds between 150- 250 mg/cc (AUC 0.68 - 0.69). When analyzing the combined dataset for men and women the strongest performance of all variables was achieved for Tb.Sp with a threshold of 150mg/cc. The other microstructural variables also showed optimum performance in the range of threshold between 120mg/cc (Tb.Th) and 250mg/cc (Tb.N). A threshold of 150 mg/cc thus appeared to permit good performance for all relevant microstructural variables and was used for all subsequent analyses.

Table 1 lists the BMD and microstructural characteristics of the different subject groups. Among single variables the best discriminatory power was achieved for Tb.Sp ($p < 0.0001$), followed by BV/TV ($p = 0.012$), BMD ($p = 0.018$), and Tb.N ($p = 0.03$). ROC and logistic regression analyses showed similar rankings: Tb.Sp with an AUC of 0.75 and OR of 2.4 (1.5 to 3.9), BV/TV with an AUC of 0.632 and OR 1.7 (1.1 to 2.5), BMD with an AUC of 0.62 and OR of 1.6 (1.1 to 2.5) and Tb.N with an AUC of 0.62 and OR of 1.6 (1.1 to 2.3). For Tb.Sp < 0.6 mm only 18% of the patients had prevalent fractures whereas at Tb.Sp > 0.75 mm the fraction rose to 68%. Cortical parameters did not differ significantly between patients with fractures and controls.

In separate analyses for men and women, Tb.Sp showed significant discriminative power for prevalent fractures for both genders, with men demonstrating 0.72 ± 0.09 (with fractures) versus 0.63 ± 0.09 (without fractures), AUC = 0.73 ± 0.07, sOR = 3.0 (1.5 to 5.6), $p < 0.01$ (Table 2). Women showed a Tb.Sp of 0.70 ± 0.10 (with fractures) versus 0.63 ± 0.11 (without fractures), AUC = 0.68 ± 0.08, sOR = 2.1 (1.1 to 4.1). Adjustment of structural variables for BMD led to a nonsignificant increase of the discriminatory power of the structural variables: adjusted OR Tb.Sp 8.4 (2.9 to 28.5), adjusted OR Tb.Th 3.6 (1.3 to 10.2), adjusted OR Tb.N 2.0 (1.3 to 3.2). In these combined models, the structural parameters remained significant predictors independent of BMD.

Figure 5 shows multivariate ROC analyses for BMD and structural variables with AUCs and levels of significance for differences between AUCs displayed. Tb.Sp alone as well as each model containing Tb.Sp showed stronger performance than BMD ($p < 0.001$). A model containing all trabecular variables, ie, trabecular BMD and all trabecular structural variables evaluated resulted in the highest AUC of 0.82, significantly stronger than Tb.

Table 1. BMD and Microstructural Characteristics for All Patients, Men and Women, Comparing Cases With Vertebral Fracture to Controls Without Such Fractures

	All patients ($n = 104$)		Women ($n = 44$)		Men ($n = 60$)	
	Vertebral fracture controls ($n = 58$)	Vertebral fracture cases ($n = 46$)	Vertebral fracture controls ($n = 22$)	Vertebral fracture cases ($n = 22$)	Vertebral fracture controls ($n = 36$)	Vertebral fracture cases ($n = 24$)
Age (years)	62.4 ± 12.6	64.3 ± 9.2	61.9 ± 12.9	65.4 ± 10.7	62.7 ± 12.5	63.3 ± 7.7
Trabecular BMD (mg/mL)	191.7 ± 50.6	$169.8 \pm 40.5^{*}$	192.5 ± 54.0	178.3 ± 34.6	191.2 ± 49.2	$162 \pm 44.5^{*}$
Cortical BMD (mg/mL)	384.1 ± 55.1	369.9 ± 39.3	375.3 ± 43.4	355.3 ± 30.8	389.5 ± 61.1	383.3 ± 42.0
BV/TV (%)	0.55 ± 0.07	$0.51 \pm 0.06^{*}$	0.55 ± 0.08	0.53 ± 0.06	0.55 ± 0.06	$0.50 \pm 0.06^{**}$
BS/BV?(%)	3.0 ± 0.49	3.1 ± 0.49	3.0 ± 0.58	3.0 ± 0.48	3.0 ± 0.43	$3.3 \pm 0.44^{**}$
Tb.Sp (mm)	0.63 ± 0.10	$0.71 \pm 0.09^{***}$	0.63 ± 0.11	$0.70 \pm 0.10^{*}$	0.63 ± 0.09	$0.72 \pm 0.09^{***}$
Tb.N (1/mm)	0.82 ± 0.05	$0.79 \pm 0.05^{*}$	0.81 ± 0.05	$0.77 \pm 0.05^{*}$	0.82 ± 0.04	0.81 ± 0.04
Tb.Th (mm)	0.68 ± 0.11	0.65 ± 0.11	0.69 ± 0.14	0.69 ± 0.11	0.67 ± 0.09	$0.61 \pm 0.09^{*}$
Ct.Th (mm)	0.22 ± 0.02	0.22 ± 0.03	0.21 ± 0.02	0.21 ± 0.02	0.24 ± 0.04	0.22 ± 0.03

Values are mean ± SD; p value comparing patients with vertebral fracture and controls with Student's t test: $^{*}p < 0.05$, $^{**}p < 0.01$, $^{***}p < 0.001$.

Sp alone ($p = 0.007$). In this model Tb.Sp, Tb.N, and Tb.Th each contributed significantly, whereas BMD and BV/TV did not. Again, gender was not a significant contribution as confounder in univariate and multivariate logistic regression models.Figure 5

Discussion

In this cross-sectional study we tested the potential for low-dose QCT bone structural analysis (LDSA) derived from regular whole-body CT scans as a method to assess fracture risk in myeloma patients. The assessment was based on loss of BMD and the numerical detection of diffuse changes of bone structure. Indeed, our results document that structural analysis is able to discriminate between patients with and without vertebral fracture. Importantly, the discriminatory power was higher than that of trabecular BMD in the same vertebra. Thus the method shows potential for identifying patients with vertebrae susceptible to fracture and potentially in need for orthopedic surgery to avoid neural complications.

Intriguingly, the higher levels of trabecular separation may indicate a process of trabecular rarefaction caused by osteolytic processes not yet visible in radiological examination. A comparison with an earlier study[23] supports this hypothesis. In a small cohort of myeloma patients, Takasu and colleagues[23] reported on characteristics of patients with MM without visible bone lesions or pathological fractures compared to healthy controls. In their report, patients with MM had lower Tb.N whereas Tb.Th and Tb.Sp were significantly increased when compared to the control group without MM, with Tb.Sp increasing by a factor of two. In our cohort a majority of patients (77 cases or 74%; data not shown) had advanced myeloma bone disease and these patients showed visible osteolytic lesions outside of the vertebral body imaged and analyzed in this study. In agreement with the results by Takasu and colleagues,[23] these changes can be interpreted as a possible correlates to osteolytic changes that were not detectable by the radiologists.

Unlike HR-QCT measurements, eg, employed by Takasu and colleagues,[23] the low-dose spiral CT scans of the whole body in our study are routine radiological investigations of myeloma patients, used for initial staging and follow-up.[34–36] Because CT studies on myeloma patients are rare, it is important to develop methods that allow for the investigation of large patient cohorts, taking into account the heterogeneity inherent to this disease. It is therefore encouraging to observe that the LDSA analysis method presented here proved to be a sensitive and adequate tool to detect fracture-relevant changes of BMD and bone structure. Bone structure variables showed significant associations with fracture prevalence, and assessment of Tb.Sp appears to be best suited for clinical fracture risk assessment.

Bone structural measurements in low-dose CT scans differ from HR-QCT scans because of the larger slice thickness and decreased radiation dose, which results in a considerable decrease of in-plane and out-of plane resolution. This lower resolution is associated with increases in partial volume effects, which cause a lower measured tissue mineral density and increased density of the marrow space between the trabecular struts. Therefore, for the assessment of trabecular bone structure, a lower threshold of 150 mg/cc was used compared to the level of 250 mg/cc used in HR-QCT studies.[25–27] We identified this threshold of 150 mg/cc by repeated analyses testing different thresholds with regard to optimal fracture

Table 2. Odds Ratios for Association With Vertebral Fractures in All Patients, Men, and Women

	All patients ($n = 104$)	Women ($n = 44$)	Men ($n = 60$)
Trabecular BMD (mg/cc)	1.6 (1.1–2.5)*	1.4 (0.8–2.6)	2.1 (1.1–3.9)*
Cortical BMD (mg/cc)	1.4 (0.9–2.1)	1.8 (0.9–3.2)	1.1 (0.7–1.9)
BV/TV (%)	1.7 (1.1–2.5)**	1.1 (0.6–2.4)	2.3 (1.2–4.2)**
BS/BV (%)	1.2 (0.8–1.8)	1.3 (0.6–2.5)	1.8 (1.1–3.3)*
Tb.Sp (mm)	2.4 (1.5–3.9)***	2.1 (1.1–4.1)*	3.0 (1.5–5.6)**
Tb.N (1/mm)	1.6 (1.1–2.4)*	2.0 (1.1–3.8)*	1.2 (0.7–2.1)
Tb.Th (mm)	1.2 (0.8–1.8)	1.0 (0.6–1.8)	1.8 (1.1–3.3)*
Ct.Th (mm)	1.1 (0.7–1.5)	1.2 (0.7–2.3)	1.2 (0.7–2.0)

Values are odds ratio (SD); p values comparing patients with vertebral fracture and controls with Student's t test: *$p < 0.05$, **$p < 0.01$, ***$p < 0.001$.

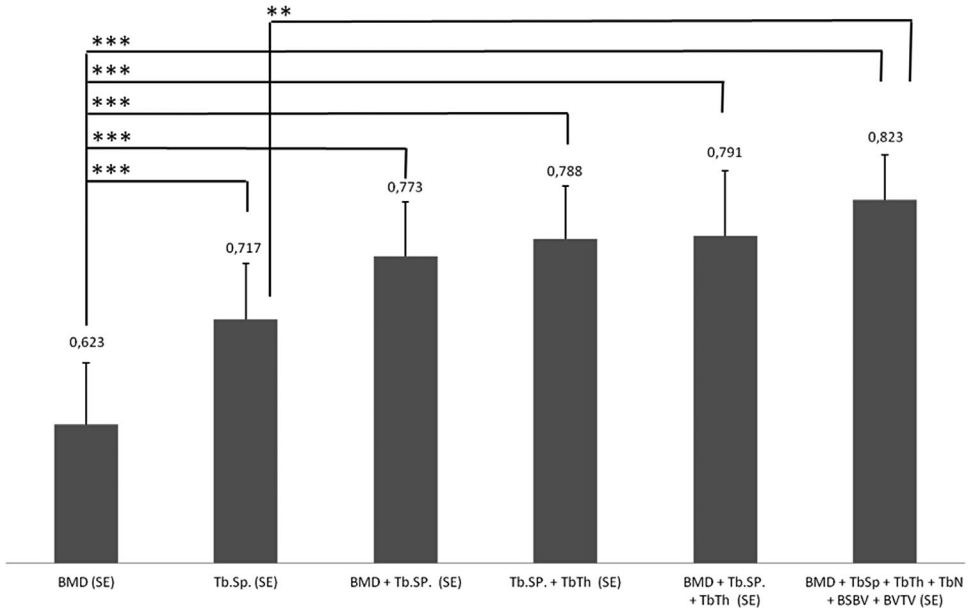

Fig. 4. AUC for the association of BMD and bone structural parameters with prevalent vertebral fractures ($n = 104$). Value of p for differences of AUC results in between the fracture discriminators in the de Long test, **$p < 0.01$, ***$p < 0.001$.

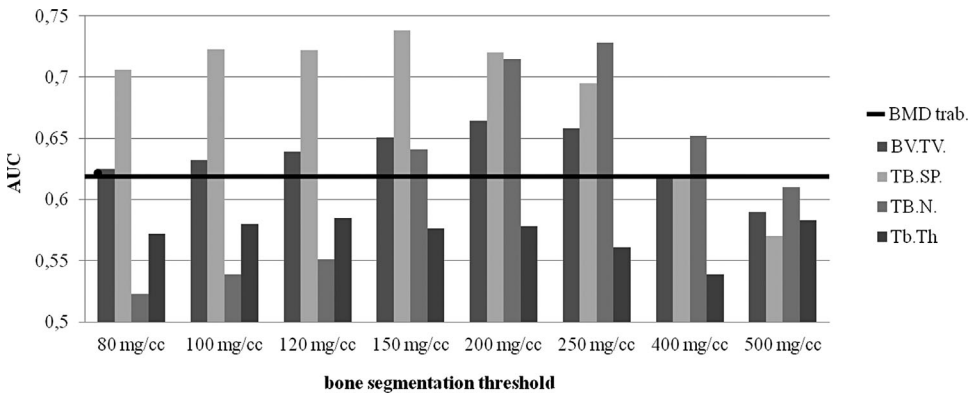

Fig. 5. AUC for the association of bone structural parameters and prevalent vertebral fractures as a function of the bone segmentation threshold used. AUC for BMD for comparison.

discrimination for trabecular separation. However, bone thresholds between 120 and 250 mg/cc showed similar performance and also appeared to be suitable.

In this study we employed a long, lightweight QCT calibration phantom that can be integrated comfortably into the clinical routine because the phantom can remain in the mat of the CT table without interfering with other clinical CT investigations conducted. We observed that the lightweight phantom tends to bend slightly because of the patient's weight. The slight resulting phantom tilt was relevant to the analysis. Geometric adaptation to the tilt was integrated into Structural*Insight* software and observed to be essential for adequate calibration. The phantom permits examination of the vertebral bodies of the entire spine over a length of 130 cm. Therefore, although beyond the goals of our study, the phantom permits investigation of any target vertebrae of clinical interest in myeloma disease or research on bone metastases, and allows testing of biomechanical stability. This might be of particular importance for studying the reported differences in fracture risk between thoracic and lumbar vertebral fractures.[34] Vertebral bodies that are being considered at high risk of fracture by clinicians, for example due to larger focal osteolytic lesions, could be investigated by LDSA in the future, to refine and objectify the level of risk. For this purpose more refined biomechanical analyses such as finite element analyses for direct calculation of bone strength under a variety of loading conditions[37,38] is possible with LDSA, as well as quantitative follow-up investigations of target lesions and bone density.

In this first study we focused on providing data that quantify vertebral fracture risk in relation to bone density and structural variables of the index vertebrae T_{11} and T_{12}. The structural variables derived performed well in fracture discrimination. All trabecular structural variables tested showed a significant OR; this was highest for the predefined endpoint variable Tb.Sp with an OR of 2.4 (AUC = 0.749). Both diffuse osteolytic lesions and osteoporotic bone loss increase Tb.Sp, and its typical magnitude on the order of a millimeter or more (much larger than the magnitude of other structural measures) make this parameter easier to measure at decreased resolution such as in LDSA. In multivariate models including the reference parameter trabecular BMD, Tb.Sp remained a significant predictor whereas BMD remained significant in women but not in men. In bivariate models, the strongest association to vertebral fractures was seen in combination of Tb.Sp and Tb.Th (AUC = 0.788). Further improvement in AUC was achieved when including BMD and the remaining trabecular structural parameters in an age-adjusted model (AUC = 0.823).

When comparing the QCT results between the genders, we observed reduced Tb.N, Tb.Th, and cortical BMD in women. In general, the structural parameters showed a somewhat stronger discrimination in men than in women, but these differences were variable and not significant. Adjustment for BMD showed stronger effects in women than in men. However, the sample size for gender-specific analyses was relatively small and thus these differences need to be verified in larger studies.

Although trabecular bone variables performed well, the cortical parameters did not provide value for vertebral fracture risk assessment. This may be because cortical thickness measures only on the order of 0.3 mm,[39] and might therefore be too thin to be assessed accurately with LDSA.

There are several limitations to this study. The cross-sectional study design shows the association to existing fractures and does not provide estimates of fracture risk. However, the results are promising for prospective trials addressing the association to fracture risk. In contrast to prospective trials in patients with osteoporosis, the incidence of fractures in patients with MM is high, and strategies to determine the individual fracture risk for primary and secondary fracture prevention are sparse.[40,41] Another limitation of LDSA in comparison to HR-QCT is reduced precision due to increased noise levels. Nevertheless, LDSA has the advantage that it administers a radiation dose of approximately 4 to 6.5 mSv for the entire body scan, whereas the dose reported for HR-QCT scans in the study by Takasu and colleagues[23] amounted to more than 20 mSv for assessment of the spine alone. A further limitation of the study is that the optimal threshold for LDSA was determined for the particular CT scanner used in our study, whereas the numerical values of the QCT measures are likely to vary across CT scanner models. Differences in in-plane resolution, slice thickness, reconstruction kernel, and beam energy would affect the measurements significantly. Thus, the largest hurdle to clinical implementation may be to calibrate the technique such that results can be consistently compared to some interventional threshold. However, the cross-calibration could be accomplished by scanning a standard QA phantom in order to adjust to the gray level and the spatial resolution of the CT scanners. Despite its limitations, our study demonstrates that LDSA is accurate enough to provide relevant data associated with fracture prevalence.

Taking advantage of our method's clinical applicability for epidemiological studies on myeloma patients, especially when compared to High Resolution CT (HRCT), a large number of questions can now be investigated. For example, to what extent diffuse bone loss and to what extent focal osteolytic lesions increase fracture risk in representative populations. It is most interesting to test whether the observed rarefaction of trabecular bone microstructure detected with our method may reflect osteolytic bone changes that are not yet visible to the investigator's eye. This needs to be explored in future studies, for example in comparison to MRI. Furthermore, the changes in microstructure could be correlated with X-ray findings and clinical endpoints such as back pain and mortality. Finally, the power for fracture discrimination of our method could be compared to DXA. In prospective studies one should examine whether fracture risk assessments for these patients can be improved beyond the simple clinical estimates currently in use.[15,17–19] LDSA allows further investigation of known differences in immunoglobulin-subtype[38] on fracture status and risk. One could also study whether there is a difference in treatment response in specific subpopulations of the disease. Finally, oncologists are interested in whether medication dose adaptations, which are meant to reduce side effects, show an effect on treatment results[10,42] and if fracture risk or disease progression can be detected early in patients with smoldering myeloma or MGUS.[5,6] The method can be refined in many ways by including new image reconstruction techniques that reduce image noise or by including finite element analyses to estimate absolute levels of bone strength.

We conclude that LDSA appears to be an effective method to perform biomechanical investigations on myeloma patients, allowing structural measures on vertebrae to be derived that permit discrimination of vertebral fracture status and which thus have the potential to be associated with future fracture risk.

Disclosures

All authors state that they have no conflicts of interest.

Acknowledgments

This work was supported by grants from Bundesministerium für Bildung und Forschung (BMBF), Germany (BioAsset grant 01EC1005 to FT and JP).

Authors' roles: JB and CCG initiated and conducted the study. MH set up the clinical setting and provided the review. SG and AG performed the clinical data assessment. SG performed LDSA measures. FT, JP, and GC programmed the innovations for the structural insight software packages. AW and JB performed fracture analysis. Analysis of data was performed by JB and CCG. JB takes responsibility for data integrity.

References

1. Raab MS, Podar K, Breitkreutz I, Richardson PG, Anderson KC. Multiple myeloma. Lancet. 2009;374: 324–39.
2. Bartl R, Fateh-Moghadam A. [The diagnosis of multiple myeloma]. Onkologie. 1986;9:183–8, 190–5.
3. Lecouvet FE, Vande Berg, Michaux BC, Jamart L, Maldague J. Malghem J Development of vertebral fractures in patients with multiple myeloma: does MRI enable recognition of vertebrae that will collapse. J Comput Assist Tomogr. 1998;22: 430–6.
4. Mahnken AH, Wildberger JE, Gehbauer G, Schmitz-Rode T, Blaum M, Fabry U, Gunther RW. Multidetector CT of the spine in multiple myeloma: comparison with MR imaging and radiography. AJR Am J Roentgenol. 2002;178: 1429–36.
5. Melton LJ 3rd, Kyle RA, Achenbach SJ, Oberg AL, Rajkumar SV. Fracture risk with multiple myeloma: a population-based study. J Bone Miner Res. 2005;20: 487–93.
6. Melton LJ 3rd, Rajkumar SV, Khosla S, Achenbach SJ, Oberg AL, Kyle RA. Fracture risk in monoclonal gammopathy of undetermined significance. J Bone Miner Res. 2004;19: 25–30.
7. Vogel MN, Weisel K, Maksimovic O, et al. Pathologic fractures in patients with multiple myeloma undergoing bisphosphonate therapy: incidence and correlation with course of disease. AJR Am J Roentgenol. 2009;193: 656–61.
8. Kyle RA, Gertz MA, Witzig TE, et al. Review of 1027 patients with newly diagnosed multiple myeloma. Mayo Clin Proc. 2003;78: 21–33.
9. Alexanian R, Haut A, Khan AU, et al. Treatment for multiple myeloma. Combination chemotherapy with different melphalan dose regimens. JAMA. 1969;208: 1680–5.
10. Barlogie B, Tricot G, Anaissie E, et al. Thalidomide and hematopoietic-cell transplantation for multiple myeloma. N Engl J Med. 2006;354: 1021–30.
11. Lahtinen R, Laakso M, Palva I, Virkkunen P, Elomaa I. Randomised, placebo-controlled multicentre trial of clodronate in multiple myeloma. Finnish Leukaemia Group. Lancet. 1992;340: 1049–52.
12. Adams J, Kauffman M. Development of the proteasome inhibitor Velcade (Bortezomib). Cancer Invest. 2004;22: 304–11.
13. Dolloff NG, Talamo G. Targeted therapy of multiple myeloma. Adv Exp Med Biol. 2013;779: 197–221.
14. Richardson PG, Lonial S, Jakubowiak AJ, Harousseau JL, Anderson KC. Monoclonal antibodies in the treatment of multiple myeloma. Br J Haematol. 2011; Sep 154:(6):745–54.
15. Delorme S, Baur-Melnyk A. Imaging in multiple myeloma. Eur J Radiol. 2009;70: 401–8.
16. Winterbottom AP, Shaw AS. Imaging patients with myeloma. Clin Radiol. 2009;64: 1–11.
17. Durie BG, Salmon SE. A clinical staging system for multiple myeloma. Correlation of measured myeloma cell mass with presenting clinical features, response to treatment, and survival. Cancer. 1975;36: 842–54.
18. Baur-Melnyk A, Reiser M. [Staging of multiple myeloma with MRI: comparison to MSCT and conventional radiography]. Radiologe. 2004;44: 874–81.
19. Ewerbeck V, Friedl W. [Surgical treatment of skeletal metastases: the surgical treatment of spinal metastases]. Berlin, Germany: Springer; 1992. p. 77–110. German.
20. Crawford RP, Cann CE, Keaveny TM. Finite element models predict in vitro vertebral body compressive strength better than quantitative computed tomography. Bone. 2003;33: 744–50.
21. Keaveny TM, Biomechanical computed, tomography-noninvasive bone, strength analysis, using clinical, computed tomography, scans. Ann N Y Acad Sci. 2010;1192: 57–65.
22. Melton LJ 3rd, Riggs BL, Keaveny TM, et al. Structural determinants of vertebral fracture risk. J Bone Miner Res. 2007;22: 1885–92.
23. Takasu M, Tani C, Ishikawa M, et al. Multiple myeloma: microstructural analysis of lumbar trabecular bones in patients without visible bone lesions—preliminary results. Radiology. 2011;260: 472–9.
24. Genant HK, Wu CY, van Kuijk C, Nevitt MC. Vertebral fracture assessment using a semiquantitative technique. J Bone Miner Res. 1993;8: 1137–48.
25. Graeff C, Chevalier Y, Charlebois M, et al. Improvements in vertebral body strength under teriparatide treatment assessed in vivo by finite element analysis: results from the EUROFORS study. J Bone Miner Res. 2009;24: 1672–80.
26. Graeff C, Marin F, Petto H, et al. High resolution quantitative computed tomography-based assessment of trabecular microstructure and strength estimates by finite-element analysis of the spine, but not DXA, reflects vertebral fracture status in men with glucocorticoid-induced osteoporosis. Bone. 2013;52: 568–77.
27. Graeff C, Timm W, Nickelsen TN, et al. Monitoring teriparatide-associated changes in vertebral microstructure by high-resolution CT in vivo: results from the EUROFORS study. J Bone Miner Res. 2007;22: 1426–33.
28. Krebs A, Graeff C, Frieling I, et al. High resolution computed tomography of the vertebrae yields accurate information on trabecular distances if processed by 3D fuzzy segmentation approaches. Bone. 2009;44: 145–52.
29. Parfitt AM, Drezner MK, Glorieux FH, et al. Bone histomorphometry: standardization of nomenclature, symbols, and units. Report of the ASBMR Histomorphometry Nomenclature Committee. J Bone Miner Res. 1987;2: 595–610.
30. Dougherty G. Medical image processing: techniques and applications. New York: Springer; 2011. p. 200.
31. Hildebrand T, Rüegsegger P. A new method for the model-independent assessment of thickness in three-dimensional images. J Microsc. 1997;185: 67–75.
32. Sieber C. Multiskalen-Frakturdiskriminierung am Humanen Wirbelkörper in vitro [Multiscale fracture discrimination on human vertebral bodies in vitro] [dissertation]. [Kiel, Germany]: Christian-Albrechts-Universität; 2006. German.
33. De Long ER, De Long DM, Clarke-Pearson DL. Comparing the areas under two or more correlated receiver operating characteristic curves: a nonparametric approach. Biometrics. 1988;44: 837–45.
34. Angtuaco EJ, Fassas AB, Walker R, Sethi R, Barlogie B. Multiple myeloma: clinical review and diagnostic imaging. Radiology. 2004;231: 11–23.
35. Horger M, Claussen CD, Bross-Bach U, et al. Whole-body low-dose multidetector row-CT in the diagnosis of multiple myeloma: an alternative to conventional radiography. Eur J Radiol. 2005;54: 289–97.
36. Horger M, Kanz L, Denecke B, et al. The benefit of using whole-body, low-dose, nonenhanced, multidetector computed tomography for follow-up and therapy response monitoring in patients with multiple myeloma. Cancer. 2007;109: 1617–26.
37. Wang X, Sanyal A, Cawthon PM, et al. Prediction of new clinical vertebral fractures in elderly men using finite element analysis of CT scans. J Bone Miner Res. 2012;27: 808–16.
38. Zysset PK, Dall'ara E, Varga P, Pahr DH. Finite element analysis for prediction of bone strength. Bonekey Rep. 2013;2: 386.
39. Amling M, Posl M, Ritzel H, et al. Architecture and distribution of cancellous bone yield vertebral fracture clues. A histomorphometric analysis of the complete spinal column from 40 autopsy specimens. Arch Orthop Trauma Surg. 1996;115: 262–9.

40. Alegre A, Gironella M, Bailen A, Giraldo P. Zoledronic acid in the management of bone disease as a consequence of multiple myeloma: a review. Eur J Haematol. 2013;92: 181–8.
41. Terpos E, Morgan G, Dimopoulos MA, et al. International Myeloma Working Group recommendations for the treatment of multiple myeloma-related bone disease. J Clin Oncol. 2013;31: 2347–57.
42. Barlogie B, Desikan R, Eddlemon P, et al. Extended survival in advanced and refractory multiple myeloma after single-agent thalidomide: identification of prognostic factors in a phase 2 study of 169 patients. Blood. 2001;98: 492–4.